Estimating Capacity Loss of Somasila Reservoir, India Using Per-Pixel and Sub-Pixel Classification Technique

Jeyakanthan V S

National Institute of Hydrology, Kakinada, A.P
E-mail: jeyakanthan05@gmail.com

ABSTRACT: *Periodic surveys of reservoirs are essential to evaluate the decrease in storage capacity due to inflow and trapping of sediment. Conventional hydro-graphic surveys are time consuming, labour intensive and expensive. Satellite remote sensing techniques provide time and cost effective approach for the periodical capacity surveys. The traditional approaches of image classification such as maximum likelihood and the band thresholding method, involve the per-pixel approach to delineate the water spread area of a reservoir. One of the limitations of these approaches is that the pixels representing the reservoir border, containing a mixture of water, soil and vegetation, are classified entirely as water, thereby resulting in, inaccurate estimate of the water spread area. To compute the water spread area accurately, the sub-pixel approach has been used in this study. The water spread areas extracted using per-pixel and sub-pixel approaches from IRS-1C and IRS-1D satellite image data were in turn used to quantify the capacity of the Somasila Reservoir, Andhra Pradesh, India. The estimated capacity of the reservoir using the per-pixel and sub-pixel approaches was 1134.16 Mm^3 and 1123.59 Mm^3, respectively. The robustness of sub-pixel approach in classifying the water spread has been evaluated by comparing it with the high resolution data. The validation shows that the sub-pixel approach produced much less error (1.08%) than the per-pixel based approach (3.14%).*

Keywords: Reservoir, Water Spread Area, Capacity Estimation, Sub-Pixel Approach.

INTRODUCTION

Sediment deposition and its accumulation in a reservoir depend on the sediment load carried by rivers and reservoir storage capacity respectively (Phatarford, 1990). Rivers in India carry only 5% of the global water runoff but they transport about 30% of the total sediment carried to the oceans (Milliman and Meade, 1983). The transported silt eventually gets deposited at different levels of a reservoir and reduces its storage capacity (Goel *et al.,* 2002, Jain *et al.,* 2002, Sreenivasulu and Udayabaskar 2010). Reduction in the storage capacity beyond a limit prevents the reservoir from the fulfillment of the purpose for which it is designed. Periodical capacity surveys of the reservoir help in assessing the rate of sedimentation and reduction in storage capacity. The conventional technique such as hydrographic survey and inflow-outflow approaches, for the estimation of capacity of a reservoir are cumbersome, time consuming, expensive and involve more man power. An alternate to conventional methods, remote

sensing technique provides cost and time effective estimation of the live capacity of a reservoir (Jain 2002).

To quantify the capacity of a reservoir, the only thematic information that has to be extracted from the satellite data is the water spread area at different water levels of the reservoir (Morris and Fan 1998, Peng 2006). Different approaches to delineate various thematic information from the remote sensing digital data, such as maximum likelihood classification, minimum distance to mean classification and the band threshold method, adopt the per-pixel based methodology and assign a pixel to a single land cover type (Jensen 1996, Bastin 1997); whereas in reality, a single pixel may contain more than one type of land cover (known as a mixed pixel). Mixed pixels are common especially near the boundaries of two or more discrete classes (Foody and Cox 1994, Shalan *et al.,* 2003, Ibrahim *et al.,* 2005). The boundary pixels of the water spread area that are mixed in nature, representing soil or vegetation with moisture, are classified as water pixels when a per-pixel based approach is applied, thereby producing an inaccurate estimate of the water spread area. To accurately compute the water spread area to the maximum possible extent, thereby reducing the error in the estimation of the capacity of a reservoir, a sub-pixel or linear mixture model (LMM) approach has been chosen for classifying the boundary pixels of the water spread area from different water levels of the Somasila Reservoir located in the Andhra Pradesh state of India.

STUDY AREA

Somasila reservoir is located on the river Pennar which flows through the Nellore district in Andhra Pradesh. The reservoir is at a distance of about 80 k.m from Nellore town which is also the district capital. The river basin receives rainfall during both the monsoon seasons (NE and SW) with major contribution from the Northeast monsoon. The normal annual rainfall at Nellore is 988 mm. The mean maximum and mean minimum temperatures are 40.9°C and 16.9°C respectively. The principal soil types in the basin are red loam, red sand, black loam and black clay. Red soils cover major portion of the basin. The general crops grown in the basin are paddy, groundnut, Bajra, Jowar, Ragi, Vegetables and Sugarcane. With the aforementioned topography, rainfall and landuse, it is evident that an appreciable amount of sediment is carried by the streams in the basin into the Somasila reservoir, thereby reducing its capacity.

Satellite Data Used

The image data used in this study were obtained by the Indian Remote Sensing (IRS) satellites IRS-1C and 1D (LISS-III sensor) which provides a spatial resolution of 24 m and spectral resolution in four different bands (0.52–0.59, 0.62–0.68, 0.77–0.86, 1.55–1.70 μm). Reservoir water level data on the day of satellite pass and the available hydrographic survey details have been collected from the Somasila Reservoir Authority responsible for collection of required data and operation of the reservoir.

METHODOLOGY

The changes in the water spread could be accurately estimated by analysing the areal spread of the reservoir at different elevations over a period of time using the satellite image data (Morris and Fan 1998, Smith and Pavelsky 2009). Per-pixel and sub-pixel approaches have been used in this study to extract the water spread area of the reservoir. Estimated water spread

areas were used in a simple volume estimation formula to compute the storage capacity of the reservoir. Estimation of the water spread area and the computation of the capacity of the reservoir are discussed in the following sections.

In the IRS-1C and 1D (LISS-III) satellite data the reservoir water spread area was free from clouds and noise for all of the seven temporal images used. All the images used in the study were geo-referenced using polyconic projection and the nearest neighbour re-sampling technique to create a geo-referenced image with a pixel size of 24 m × 24 m. In every image, 25 to 30 ground control points were used, which resulted in a root mean squared error (RMSE) of 0.15 to 0.2 of a pixel.

Per–Pixel Based Approach

Water reflects most of the visible wavelengths, but the energy at the near-infrared (NIR) wavelength is almost absorbed by the water, thus providing a good contrast between land and water in the NIR images (Lillesand and Kiefer 1994). Such a contrast helps in extracting the water-spread area of the reservoir. Different procedures have been adopted by many researchers (McFeeters 1996, Fraser and Page 2000, Chopra *et al.,* 2001, Toyra *et al.,* 2001, Jain *et al.,* 2002, Rathore 2006) for water body identification in wetland areas and reservoirs, which adopts the per-pixel based approach. Among them the band threshold approach is easy and valid method for identifying the water body. Also it has been suggested that this per-pixel based approach could give good estimates of the area of water body if NIR band is used (Goel 1996, Jain 2002, Hui 2008). In addition, the panchromatic image data used for validation can be processed only by band threshold approach. Therefore, in the per-pixel based approach band threshold technique was adopted to extract the water pixels that correspond to various water levels of the reservoir. The following model equation has been used in the image processing software to delineate the water-spread area of the reservoir. The adopted algorithm states that:

if

$$P_{V-NIR} > T_{L-NIR} \text{ and} \hspace{4cm} \text{… (1)}$$

$$P_{V-NIR} < T_{H-NIR} \text{ then}$$

the pixel is in the water-spread area, where, P_{V-NIR} is the pixel value in NIR band, T_{L-NIR} and T_{H-NIR} are lower and higher thresholds for the NIR band.

Sub–Pixel Based Approach

The sub-pixel classifier uses the linear unmixing technique that allows for the identification of the "material of interest" and the determination of its "material part fraction" or cover percentage within a pixel. Linear spectral unmixing is a perfect approximation for calculating the abundance or fraction of an end-member in an image pixel. The LMM classification technique attempts to estimate the proportions of specific classes that occur within each pixel using the linear mixing approach (Foody 1996, Aplin and Atkinson 2001, Min Xu 2005). In this study, the reservoir water spread area was estimated using the linear spectral unmixing approach.

The basic assumption of the LMM is that the measured reflectance of a pixel is the linear sum of the reflectance of the components that make up the pixel. The basic hypothesis is that the image spectra are the result of mixtures of surface materials, shade and clouds and that each

of these components is linearly independent from the others (Bosdogianni *et al.,* 1997, Atkinson 1997, Robert *et al.,* 1998). Linear unmixing also assumes that all of the materials within the image have sufficient spectral contrast to allow their separation. In a soft classification, the estimated variables (the fractions or proportions of each land cover class) are continuous, ranging from 0 to 100 percent coverage within a pixel. Settle and Drake (1993) and Foody and Cox (1994) proposed a mathematical expression for linear spectral unmixing. The theory behind this is that a series of end-members present within a pixel contribute to the overall spectral signature of that pixel. Hence, the spectral signature of a pixel would be derived from the sum of the products of the single spectrum of each end-member it contains, each weighted by a fraction, plus a residue as explained by the following mathematical model:

$$R_i = \sum f_k \, R_{ik} + E_i \qquad \qquad \text{… (2)}$$

where $\sum f_k = 1$ $\qquad \qquad \text{… (3)}$

and $0 \leq f_k \leq 1$ $\qquad \qquad \text{… (4)}$

> i = 1, . . ., m (number of spectral bands)
> k = 1,. . ., n (number of end-members)
> R_i = Spectral reflectance of band i of a pixel which contains one or more end-members
> f_k = Proportion of end-member k within the pixel
> R_{ik}= Known spectral reflectance of end-member k within the pixel in band i
> E_i = Error for band i (Difference between the observed pixel reflectance R_i and the reflectance of that pixel computed from the model).

Equations 2 and 3 introduce the constraints that the sums of the fractions are equal to one and they are non-negative. To solve for f_k, the following conditions must be satisfied: (i) selected end-members should be independent of each other, (ii) the number of end-members should be less than or equal to the spectral bands used, and (iii) selected spectral bands should not be highly correlated.

The sub-pixel based approach was applied to determine the proportion or fraction of the water class that exits in the peripheral pixels of the reservoir. The first step executed in the sub-pixel approach was the selection of the pure pixels (known as end-members) belonging to a specific class. In general, the border pixels may contain any combination and proportion of water, vegetation and soil classes. Hence, these three classes were chosen to represent the end-members. The scatter plot method was used to identify the end-members. The locations of the end-members in the image data were identified from the extremes of the scatter plot. The identified end-member spectra were supplied as input to the LMM approach. The output of the model run contains three images labelled as water-, soil- and vegetation- fraction images.

Computation of Volume between Successive Water Levels

Traditionally the reservoir volume between two consecutive reservoir water levels was computed using the prismoidal formula, the Simpson formula or the trapezoidal formula (Patra 2001). Of these, the trapezoidal formula has been most widely used for the

computation of volume (Goel and Jain 1996, Morris and Fan 1998, Rathore 2006). The water spread area estimated using the per-pixel and sub-pixel approaches were separately used as an input to the volume estimation formula to determine the volume at different water levels of the reservoir. In this study the volume between two consecutive reservoir water levels was computed using the following trapezoidal formula:

$$V = H \times (A1 + A2 + \sqrt{(A1 \times A2)})/3 \qquad \qquad \dots (5)$$

where V is the volume between any two consecutive water levels, A1 and A2 are the water spread areas at the reservoir water levels 1 and 2 respectively and H is the difference between these two water levels.

Computation of Storage Capacity of the Reservoir

The volumes computed (using equation 6) between different water levels (i.e., from minimum draw down level (MDDL) to Full Reservoir Level (FRL)) were added together to calculate the cumulative or storage capacity of the reservoir.

Estimating Capacity Loss Due to Sedimentation

Capacities calculated using equation (5) between the consecutive levels is added up so as to arrive at the cumulative capacity of the reservoir. The difference between the any pervious and revised cumulative capacities represents the loss in capacity of the reservoir due to sedimentation.

RESULTS AND DISCUSSION

Computation of Reservoir Capacity by the Per–Pixel Approach

Seven different water levels which vary from 82.3 m (MDDL) to 94.39 m (Near FRL) of the reservoir were selected based on the availability of cloud free satellite data to estimate the water-spread of the reservoir. The designed FRL of the reservoir is 100.584 m. To extract the water pixels from the images using per-pixel approach, algorithm (Equation 1) was used. It requires separate minimum and maximum threshold digital number (DN) from the NIR band for the seven satellite images used in the study. With the help of the algorithm, the pixels which contain, DN between the given minimum and maximum threshold values were labelled as water pixels. The lower (16) and higher (49) DN values can be attributed to the irradiance of the water-body during winter and summer season of study area. The extracted minimum DN were 16, 18, 24, 29, 29, 18 and 17 for the images pertaining to the month January, March, April, May, June, September and November respectively. The maximum pixel values were 35, 38, 40, 45, 49, 41 and 37 for the images pertaining to the month of January, March, April, May, June, September and November respectively.

The total number of water pixels that were extracted was multiplied by the area (24 m × 24 m) of a single pixel to compute the water spread area pertaining to a single image. The same technique was adopted to convert the extracted water pixels into the water spread area in all seven images used in this study.

The water spread area thus estimated in each image using the per-pixel approach has been used as an input to the trapezoidal formula (Equation 5) to calculate the consecutive volumes of the reservoir. The estimated cumulative capacity of the reservoir at a water level of 94.39 m (near FRL) using the per-pixel classification approach was 1134.16 Mm^3. Thus, the per-pixel approach was adopted and the capacity was estimated is shown in Table 2. To compare the efficiency of this method with that of the sub-pixel approach, another set of experiments was carried out, as described in the following section.

Computation of Reservoir Capacity by the Sub–Pixel Approach

The fraction images (Figure 3 and 3a) generated using the sub-pixel approach described in the Methodology section contain a wealth of information about the reservoir. Each fraction image corresponds to a single type of land cover only. For example, the pixels in the water fraction image provide information only on the proportion or amount of water contained in the pixel.
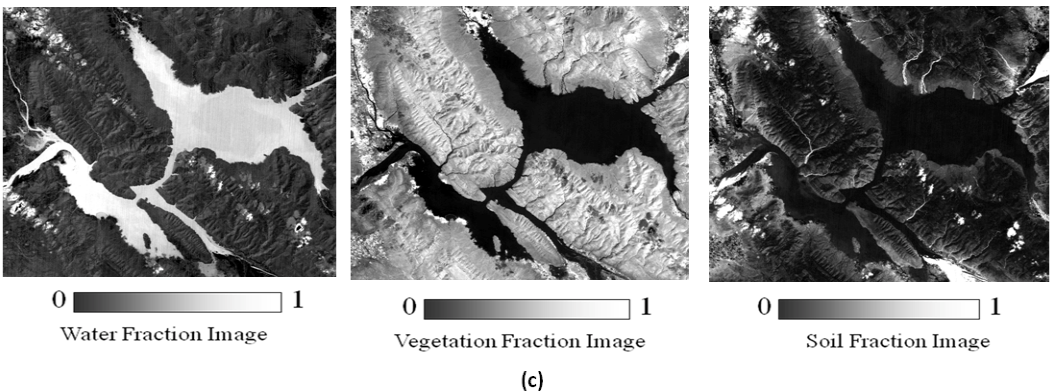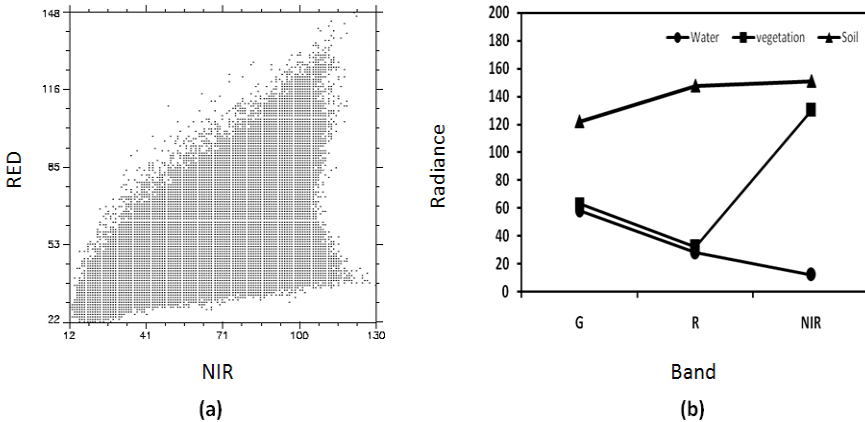

(a)

(b)

(c)

Fig. 1: (a) Feature space plot (NIR Vs RED), (b) End-member spectra of Soil, Water and Vegetation (c) Fraction images obtained by spectral unmixing of image data pertaining to the highest water level (94.39 m)
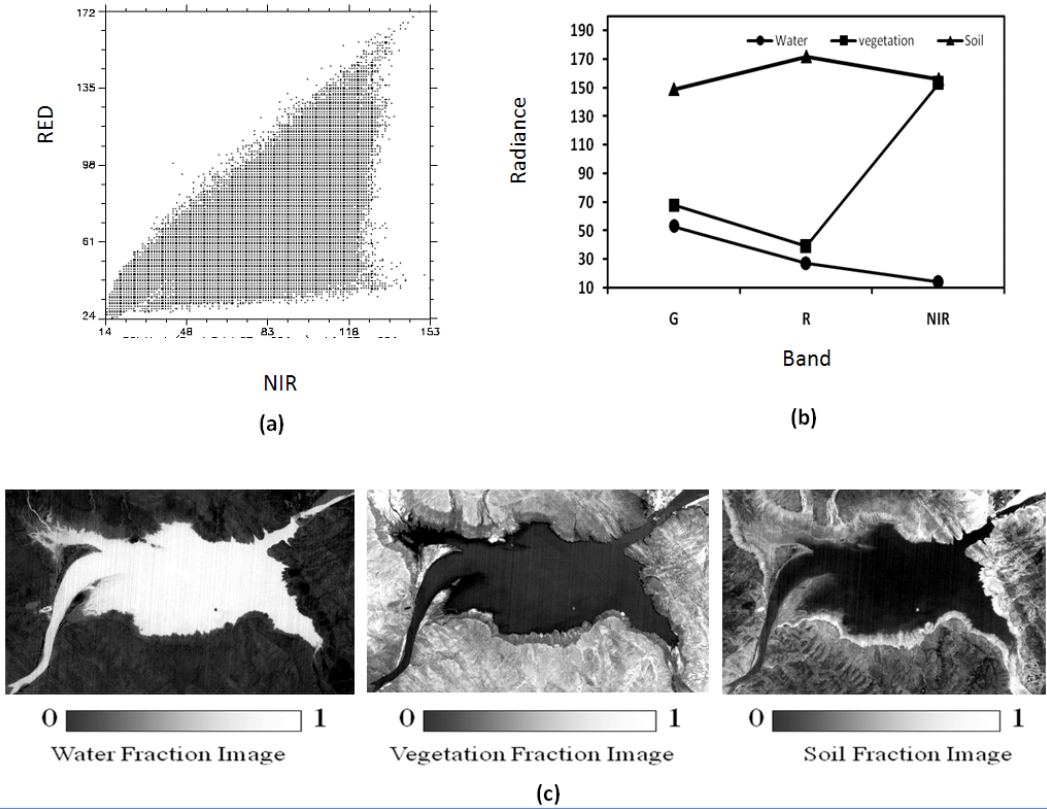
(a)

(b)

0 ⟦ ⟧ 1
Water Fraction Image

0 ⟦ ⟧ 1
Vegetation Fraction Image

0 ⟦ ⟧ 1
Soil Fraction Image

(c)

Fig. 2: (a) Feature space plot (NIR Vs RED, (b) End-member spectra of Soil, Water and Vegetation (c) Fraction images obtained by spectral unmixing of image data pertaining to the lowest water level (83.17 m)

Likewise, the vegetation and soil fraction images provide information on the proportions of their respective classes only. However, in this study the interest is only to determine the amount of water present in the border pixels of the reservoir. The value of the pixels in the fraction image ranges from 0 to 1. A pixel from the water fraction image having a value of 0 indicates that there is no water at all in that pixel, whereas a pixel having a value of 0.3 indicates that 30% of the area of the pixel is occupied by water while a pixel value of 1 indicates that 100% of the area of the pixel is occupied by water (i.e., the pixel is fully occupied by water). Therefore, for a pixel having a value of 0.65, the area of water occupied by that pixel is 374.4 m^2 (0.65 × 24 m × 24 m).

The pixels representing the peripheral portion of the reservoir, which have a minimum value of 0.1 in the water fraction image (i.e., a pixel with a minimum of 10% of its area containing water) were isolated from the water-fraction image and the area covered by water in these peripheral/border pixels was estimated. After examining the peripheral pixels it was ascertained that none of the border pixels contain water spread area less than 10%. Hence, a threshold value of 10% was selected and used for analysis. The number of pixels that contain 100% water was also determined. By summing the area occupied by these two types of pixels, the total water spread area corresponding to a particular water level of the reservoir was

computed. This exercise was carried out for each of the six images used in the study. The water spread area thus estimated was again used as an input to the trapezoidal formula to compute the storage capacity or cumulative capacity of the Somasila Reservoir using the sub-pixel classification approach.

Table 2: Capacity Loss Estimation of the Somasila Reservoir Using
Per-Pixel and Sub-Pixel Based Approaches

Date of Satellite Pass	Reservoir Elevation above m.s.l (m)	Water Spread Area (Mm²)			Cumulative Volume (Mm³)		
		Original Area (1987)	Per-Pixel Approach (2002)	Sub-Pixel Approach (2002)	Original Volume (1987)	Per-Pixel Approach (2002)	Sub-Pixel Approach (2002)
17.01.2002	94.39	118.73	118.18	116.04	1158.12	1134.16	1123.59
22.03.2002	93.47	114.82	112.69	110.73	1050.69	1027.94	1019.29
16.04.2002	92.10	104.39	102.62	101.07	900.59	880.54	874.25
11.05.2002	90.14	86.11	85.92	85.12	714.18	696.01	692.02
05.06.2002	88.30	76.38	71.82	71.00	564.78	551.09	548.58
27.11.2002	85.69	58.49	56.39	56.01	389.29	384.18	383.22
13.09.2002	83.17	47.98	46.04	45.65	255.35	255.35	255.35

It is worth mentioning that a pixel containing 65% water may be labelled as containing 100% water by the per-pixel approach. Thus, the water spread area is overestimated. Conversely, if the pixel contains 40% water then the entire pixel is not considered for the water spread area estimation. Hence, the water spread area is underestimated. Such errors due to overestimation or underestimation do not occur in the sub-pixel approach. Thus, the sub-pixel approach reduces the error imposed by the per-pixel approach. The estimated cumulative capacity of the reservoir at a water level of 94.39 m (near FRL) using the sub-pixel approach was 1123.59 Mm³. The capacity estimated using the sub-pixel approach is given in Table 2.

Estimation of Loss in Capacity

The difference between the original (1987) and revised cumulative capacity (2002) represents the loss of capacity due to sedimentation. The results show that the volume of sediment deposition by per-pixel and sub-pixel approaches were 23.96 M cum (1158.12–1134.16) and 34.53 M cum (1158.12–1123.59) respectively for the period 1987 to 2002. If a uniform rate of sedimentation is assumed in 15 years of operation of the reservoir then the sedimentation rate by per-pixel and sub-pixel approaches were 1.597 M cum and 2.30 M cum per year respectively.

Validation of the Per–Pixel and Sub–Pixel Approaches

Several investigators (Quaramby *et al.,* 1992, Oleson *et al.,* 1994, Haertel *et al.,* 2004, Foody 2007) have shown that the recovery of sub-pixel information from medium resolution data is feasible, and this information can be directly compared to that obtained at higher scales. In line with the above findings, it was decided to validate the result of the sub-pixel classification

approach (which was carried out using the 24 m resolution image data) using high resolution image data with a spatial resolution of 5 m (re-sampled IRS 1C-PAN). However, concurrent high resolution data was not available for any of the seven images used in the study. Therefore, three new sets of image data pertaining to Singoor reservoir located in Andhra Pradesh were procured in such a way that for a particular water level of the reservoir, both the 24 m and 5 m resolution image data were available. The band threshold and sub-pixel classification techniques were again carried out on the new 24 m resolution image data sets. The high resolution PAN data were classified using the band threshold method. The results of these two experiments are given in Table 3. By analysing the results for all three sets of images, it was ascertained that the band threshold method applied to the 24 m resolution image data overestimates whereas the sub-pixel method underestimates the water spread area when compared to the high resolution (5 m) data. To select the best approach the percentage of error between both these approaches were calculated. For example the percentage of error for validation 2 was calculated as follow: $((104.89–107.49)/107.49) \times 100 = 2.42\%$ and $((106.73–107.49)/107.49) \times 100 = 0.71\%$. Results of percentage of error between per-pixel and sub-pixel approaches are given in Table 4. Analysis of Table 4 reveals that the sub-pixel approach produced much less error (1.08%) than the band threshold/per-pixel approach (3.14%). This shows that the sub-pixel based approach can be applied to estimate the capacity of other reservoirs with higher accuracy than the per-pixel approach.

Table 3: Validation of the Per-Pixel and Sub-Pixel Approaches

Satellite/Sensor	IRS-P6/LISS-III (24 m)		IRS-1C/PAN (5m)
Date of Satellite Pass	Water Spread area Per-Pixel (Mm^2)	Water Spread Area Sub-Pixel (Mm^2)	Water Spread Area Per-Pixel (Mm^2)
03 Feb 2006 (Validation-1)	123.73	118.69	119.82
23 Mar 2006 (Validation-2)	104.89	106.73	107.49
15 Jan 2005 (Validation-3)	42.04	39.68	40.32

Table 4: Percentage (%) of Error between the Per-Pixel
and Sub-Pixel Based Approaches

No. of Validation	Processing Approach	
	Per-Pixel	Sub-Pixel
Validation-1	3.26%	0.94%
Validation-2	2.42%	0.71%
Validation-3	3.75%	1.58%
Average Error	**3.14%**	**1.08%**

CONCLUSION

In this study both the per-pixel and sub-pixel approaches have been performed to extract the water spread area of the reservoir using medium resolution multi-spectral image data and the

results were validated using high resolution panchromatic image data. The validation shows that the application of the sub-pixel approach produced much less error (1.08%) than the per-pixel (3.14%) based approach. The relatively lower error shown by the sub-pixel approach presents a potential use of the technology for the estimation of other reservoirs with acceptable accuracy.

Although the sub-pixel approach was found to be a better alternative than the per-pixel approach, there are certain limitations to the method, such as the fact that the spatial locations of the various fractions within a pixel are unknown. In addition, the sub-pixel classifier produces more accurate results only with hyperspectral images. Hence, the use of hyperspectral image data with higher spatial resolution would have yielded better results.

REFERENCES

Aplin, P. and Atkinson, P.M. (2001). Sub-pixel land cover mapping for per-field classification. *International Journal of Remote Sensing*, 22 (14), 2853–2858.

Atkinson, P.M. (1997). Mapping sub-pixel proportional land cover with AVHRR imagery. *International Journal of Remote Sensing*, 18 (4), 917–935.

Bastin, L. (1997). Comparison of fuzzy c-means classification, linear mixture modelling and MLC probabilities as tools for unmixing coarse pixels. *International Journal of Remote Sensing*, 18 (17), 3629–3648.

Bosdogianni, P., Petrou, M. and Kittler, J. (1997). Mixed pixel classification with robust statistics. *IEEE Transactions on Geoscience and Remote Sensing*, 35(3), 551–559.

Chopra, R., Verma, V.K. and Sharma, P.K. (2001). Mapping, monitoring and conservation of Harike wetland ecosystem, Punjab, India through remote sensing. *International Journal of Remote Sensing*, 22(1), 89–98.

Foody, G.M. and Cox, D.P. (1994). Sub-pixel land cover composition estimation using a linear mixture model and fuzzy membership functions. *International Journal of Remote Sensing,* l5 (3), 619–631.

Foody, G.M. (1996). Approaches for the production and evaluation of fuzzy land cover classifications from remotely sensed data. *International Journal of Remote Sensing,* 17 (7), 1317–1340.

Foody, G.M. (2007). Variability in soft classification prediction and its implications for sub-pixel scale change detection and super resolution mapping. *Photogrammetric Engineering and Remote Sensing,* 73, 923–933.

Goel, M.K. and Jain, S.K. (1996). Evaluation of reservoir sedimentation using multi-temporal IRS-1A LISS II data. *Asian Pacific Remote Sensing and GIS Journal,* 8(2), 39–43.

Goel, M.K., Jain, S.K. and Agarwal, P.K. (2002). Assessment of sediment deposition rate in Bargi Reservoir using digital image processing, *Hydrological Sciences Journal*, 47(S), S81–S92.

Ibrahim, M.A., Arora, M.K. and Ghosh, S.K. (2005). Estimating and Accommodating uncertainties through soft classification of remote sensing data, *International Journal of Remote Sensing*, 26(14), 2995–3007.

Jain, S.K., Singh, P. and Seth, S.M. (2002). Assessment of sedimentation in Bhakra Reservoir in the western Himalayan region using remotely sensed data. *Hydrological Sciences Journal,* 47 (2), 203–212.

Jensen, R.J. (1996). Introductory Digital Image Processing: A remote sensing perspective, 2nd edition (London: Prentice Hall International Ltd.).

Lillesand, T.M. and Kiefer, R.W. (1994). Remote Sensing and Image Interpretation, 3rd edition (New York: John Wiley and Sons).

Min Xu, Watanachaturaporn, P., Varshney, P.K. and Arora, M.K. (2005). Decision Tree Regression for Soft Classification of Remote Sensing Data, *Remote Sensing of Environment*, 97 (3), 322–336.

Morris, G.L. and Fan Jiahua (1998). Reservoir Sedimentation Handbook (New York: McGraw-Hill Book Co).

Patra, K.C. (2001). Hydrology and Water Resources Engineering (New Delhi: Narosa Publishing House).

Phatarford, R.M. (1990), Hydraulic Engineering, Volume 1, Proceedings of the 1990 National Conference.

Rathore, D.S., Anju, Choudhary and Agarwal, P.K. (2006). Assessment of sedimentation in Harakud Reservoir using digital remote sensing technique. *Journal of the Indian Society of Remote Sensing,* 34, 344–383.

Robert, D.A., Gardener, M., Church, R., Ustin, S., Scheer, G. and Green, R.O. (1998). Mapping Chaparral in the Santa Monica Mountains using Multiple End member Spectral Mixture Analysis. *Remote Sensing of Environment*, 65, 267–279.

Settle, J.J. and Drake, N.A. (1993). Linear mixing and the estimation of ground cover proportions. *International Journal of Remote Sensing*, 14(6), 1159–1177.

Shalan, M.A., Arora, M.K. and Ghosh, S.K. (2003). An evaluation of fuzzy classifications from IRS 1C LISS III data. *International Journal of Remote Sensing*, 23(15), 3179–3186.

Sreenivasulu, V. and Udayabaskar, P. (2010). An integrated approach for prioritization of reservoir catchment using remote sensing and geographic information system, *Geocarto International,* 25 (2), 149–168.

Toyra, J., Pietroniro, A. and Martz, L.W. (2001). Multisensor hydrologic assessment of a freshwater wetland. *Remote Sensing of Environment,* 75 (2), 162–173.